

Dynamics of the $^{16}\text{O}(e, e'p)$ Reaction at High Missing Energies

N. Liyanage,¹⁷ B. D. Anderson,¹³ K. A. Aniol,² L. Auerbach,²⁹ F. T. Baker,⁷ J. Berthot,¹ W. Bertozzi,¹⁷ P.-Y. Bertin,¹ L. Bimbot,²² W. U. Boeglin,⁵ E. J. Brash,²⁴ V. Breton,¹ H. Breuer,¹⁶ E. Burtin,²⁶ J. R. Calarco,¹⁸ L. Cardman,³⁰ G. D. Cates,²³ C. Cavata,²⁶ C. C. Chang,¹⁶ J.-P. Chen,³⁰ E. Cisbani,¹² D. S. Dale,¹⁴ R. De Leo,¹⁰ A. Deur,¹ B. Diederich,²¹ P. Djawotho,³³ J. Domingo,³⁰ B. Doyle,¹⁴ J.-E. Ducret,²⁶ M. B. Epstein,² L. A. Ewell,¹⁶ J. M. Finn,³³ K. G. Fissum,¹⁷ H. Fonvieille,¹ B. Frois,²⁶ S. Frullani,¹² J. Gao,¹⁷ F. Garibaldi,¹² A. Gasparian,^{8,14} S. Gilad,¹⁷ R. Gilman,^{25,30} A. Glamazdin,¹⁵ C. Glashauser,²⁵ J. Gomez,³⁰ V. Gorbenko,¹⁵ T. Gorringer,¹⁴ F. W. Hersman,¹⁸ R. Holmes,²⁸ M. Holtrop,¹⁸ N. d'Hose,²⁶ C. Howell,⁴ G. M. Huber,²⁴ C. E. Hyde-Wright,²¹ M. Iodice,¹² C. W. de Jager,³⁰ S. Jaminion,¹ M. K. Jones,³³ K. Joo,³² C. Jutier,^{1,21} W. Kahl,²⁸ S. Kato,³⁴ J. J. Kelly,¹⁶ S. Kerhoas,²⁶ M. Khandaker,¹⁹ M. Khayat,¹³ K. Kino,³¹ W. Korsch,¹⁴ L. Kramer,⁵ K. S. Kumar,²³ G. Kumbartzki,²⁵ G. Laveissière,¹ A. Leone,¹¹ J. J. LeRose,³⁰ L. Levchuk,¹⁵ M. Liang,³⁰ R. A. Lindgren,³² G. J. Lolos,²⁴ R. W. Lourie,²⁷ R. Madey,^{8,13,30} K. Maeda,³¹ S. Malov,²⁵ D. M. Manley,¹³ D. J. Margaziotis,² P. Markowitz,⁵ J. Martino,²⁶ J. S. McCarthy,³² K. McCormick,²¹ J. McIntyre,²⁵ R. L. J. van der Meer,²⁴ Z.-E. Meziani,²⁹ R. Michaels,³⁰ J. Mougey,³ S. Nanda,³⁰ D. Neyret,²⁶ E. A. J. M. Offermann,³⁰ Z. Papandreou,²⁴ C. F. Perdrisat,³³ R. Perrino,¹¹ G. G. Petratos,¹³ S. Platchkov,²⁶ R. Pomatsalyuk,¹⁵ D. L. Prout,¹³ V. A. Punjabi,¹⁹ T. Pussieux,²⁶ G. Quémener,³³ R. D. Ransome,²⁵ O. Ravel,¹ Y. Roblin,¹ R. Roche,⁶ D. Rowntree,¹⁷ G. A. Rutledge,³³ P. M. Rutt,³⁰ A. Saha,³⁰ T. Saito,³¹ A. J. Sarty,⁶ A. Serdarevic-Offermann,²⁴ T. P. Smith,¹⁸ A. Soldi,²⁰ P. Sorokin,¹⁵ P. Souder,²⁸ R. Suleiman,¹³ J. A. Templon,⁷ T. Terasawa,³¹ L. Todor,²¹ H. Tsubota,³¹ H. Ueno,³⁴ P. E. Ulmer,²¹ G. M. Urciuoli,¹² P. Vernin,²⁶ S. van Verst,¹⁷ B. Vlahovic,^{20,30} H. Voskanyan,³⁵ J. W. Watson,¹³ L. B. Weinstein,²¹ K. Wijesooriya,³³ R. Wilson,⁹ B. Wojtsekhowski,³⁰ D. G. Zainea,²⁴ V. Zeps,¹⁴ J. Zhao,¹⁷ and Z.-L. Zhou¹⁷

(The Jefferson Lab Hall A Collaboration)

¹Université Blaise Pascal/IN2P3, F-63177 Aubière, France

²California State University, Los Angeles, California 90032

³Institut des Sciences Nucléaires, F-38026 Grenoble, France

⁴Duke University, Durham, North Carolina 27706

⁵Florida International University, Miami, Florida 33199

⁶Florida State University, Tallahassee, Florida 32306

⁷University of Georgia, Athens, Georgia 30602

⁸Hampton University, Hampton, Virginia 23668

⁹Harvard University, Cambridge, Massachusetts 02138

¹⁰INFN, Sezione di Bari and University of Bari, I-70126 Bari, Italy

¹¹INFN, Sezione di Lecce, I-73100 Lecce, Italy

¹²INFN, Sezione Sanità and Istituto Superiore di Sanità, Laboratorio di Fisica, I-00161 Rome, Italy

¹³Kent State University, Kent, Ohio 44242

¹⁴University of Kentucky, Lexington, Kentucky 40506

¹⁵Kharkov Institute of Physics and Technology, Kharkov 310108, Ukraine

¹⁶University of Maryland, College Park, Maryland 20742

¹⁷Massachusetts Institute of Technology, Cambridge, Massachusetts 02139

¹⁸University of New Hampshire, Durham, New Hampshire 03824

¹⁹Norfolk State University, Norfolk, Virginia 23504

²⁰North Carolina Central University, Durham, North Carolina 27707

²¹Old Dominion University, Norfolk, Virginia 23529

²²Institut de Physique Nucléaire, F-91406 Orsay, France

²³Princeton University, Princeton, New Jersey 08544

²⁴University of Regina, Regina, Saskatchewan, Canada S4S 0A2

²⁵Rutgers, The State University of New Jersey, Piscataway, New Jersey 08854

²⁶CEA Saclay, F-91191 Gif-sur-Yvette, France

²⁷State University of New York at Stony Brook, Stony Brook, New York 11794

²⁸Syracuse University, Syracuse, New York 13244

²⁹Temple University, Philadelphia, Pennsylvania 19122

³⁰Thomas Jefferson National Accelerator Facility, Newport News, Virginia 23606

³¹Tohoku University, Sendai 980, Japan

³²University of Virginia, Charlottesville, Virginia 22901

³³College of William and Mary, Williamsburg, Virginia 23187

³⁴Yamagata University, Yamagata 990, Japan
³⁵Yerevan Physics Institute, Yerevan 375036, Armenia
(Received 7 September 2000)

We measured the cross section and response functions for the quasielastic $^{16}\text{O}(e, e'p)$ reaction for missing energies $25 \leq E_m \leq 120$ MeV at missing momenta $P_m \leq 340$ MeV/c. For $25 < E_m < 50$ MeV and $P_m \approx 60$ MeV/c, the reaction is dominated by a single $1s_{1/2}$ proton knockout. At larger P_m , the single-particle aspects are increasingly masked by more complicated processes. Calculations which include pion exchange currents, isobar currents, and short-range correlations account for the shape and the transversity, but for only half of the magnitude of the measured cross section.

DOI: 10.1103/PhysRevLett.86.5670

PACS numbers: 25.30.Fj, 27.20.+n

The $(e, e'p)$ reaction in quasielastic kinematics ($\omega \approx Q^2/2m_p$) [1] has long been a useful tool for the study of nuclear structure. $(e, e'p)$ cross section measurements have provided both a wealth of information on the wave function of protons inside the nucleus and stringent tests of nuclear theories. Response function measurements have provided detailed information about the different reaction mechanisms contributing to the cross section.

In the first Born approximation, the unpolarized $(e, e'p)$ cross section can be separated into four independent response functions, R_L (longitudinal), R_T (transverse), R_{LT} (longitudinal-transverse), and R_{TT} (transverse-transverse) [2,3]. These response functions contain all the information that can be extracted from the hadronic system using the $(e, e'p)$ reaction.

The first $(e, e'p)$ energy and momentum distributions were measured by Amaldi *et al.* [4]. These results, and the many others that followed them [3,5,6], were interpreted in terms of single-particle knockout from nuclear valence states despite cross sections that were about 40% lower than expected. A series of $^{12}\text{C}(e, e'p)$ experiments performed at MIT-Bates [7–11] measured much larger cross sections at high missing energy than expected by single-particle knockout models. Ulmer *et al.* [7] reported a substantial increase in the transverse-longitudinal difference, $(S_T - S_L)$, above the two-nucleon emission threshold in $^{12}\text{C}(e, e'p)$. ($S_X = \sigma_{\text{Mott}} V_X R_X / \sigma_X^{ep}$, where $X \in \{T, L\}$, and σ_X^{ep} is calculated from the off-shell ep cross section obtained using deForest's cc1 prescription [12,13].) Similar R_T/R_L enhancement has also been observed by Lanen *et al.* for ^6Li [14], by van der Steenhoven *et al.* for ^{12}C [15] and, more recently, by Dutta *et al.* for ^{12}C , ^{56}Fe , and ^{197}Au [16].

There have been several theoretical attempts [17–19] to explain the continuum strength using two-body knockout models and final-state interactions, but no single model has been able to explain all the data.

In this first Jefferson Lab Hall A experiment [20], we studied the $^{16}\text{O}(e, e'p)$ reaction in the quasielastic region at $Q^2 = 0.8$ (GeV/c)² and $\omega = 439$ MeV ($|\vec{q}| \approx 1$ GeV/c). We extracted the R_L , R_T , and R_{LT} response functions from cross sections measured at several beam energies, electron angles, and proton angles for $P_m \leq 340$ MeV/c. This paper reports the results for

$E_m > 25$ MeV; p -shell knockout region ($E_m < 20$ MeV) results from this experiment were reported in [21].

We scattered the ~ 70 μA continuous electron beam from a waterfall target [22] with three foils, each ~ 130 mg/cm² thick. We detected the scattered electrons and knocked-out protons in the two high resolution spectrometers (HRS_e and HRS_h). The details of the Hall A experimental setup are given in [23,24].

We measured the $^{16}\text{O}(e, e'p)$ cross section at three beam energies, keeping $|\vec{q}|$ and ω fixed in order to separate response functions and understand systematic uncertainties. Table I shows the experimental kinematics.

The accuracy of a response-function separation depends on precisely matching the values of $|\vec{q}|$ and ω for different kinematic settings. In order to match $|\vec{q}|$, we measured $^1\text{H}(e, ep)$ (also using the waterfall target) with a pinhole collimator in front of the HRS_e. The momentum of the detected protons was thus equal to \vec{q} . We determined the $^1\text{H}(e, ep)$ momentum peak to $\frac{\delta p}{p} = 1.5 \times 10^{-4}$, allowing us to match $\frac{\delta|\vec{q}|}{|\vec{q}|}$ to 1.5×10^{-4} between the different kinematic settings. Throughout the experiment, $^1\text{H}(e, e)$ data, measured simultaneously with $^{16}\text{O}(e, e'p)$, provided a continuous monitor of both luminosity and beam energy.

The radiative corrections to the measured cross sections were performed by two independent methods: using the code RADCOR [24,25] which unfolds the radiative tails in (E_m, P_m) space, and using the code MCEEP [26] which simulates the radiative tail based on the prescription of Borie and Drechsel [27]. The corrected cross sections obtained by the two methods agreed within their mutual statistics. The radiative corrections in the continuum amount to 10%–15% of the cross section.

At $\theta_{pq} = \pm 8^\circ$, R_{LT} extracted independently at beam energies of 1.643 and 2.442 GeV agree well within statistical uncertainties. This indicates that the systematic uncertainties are smaller than the statistical uncertainties.

TABLE I. Experimental kinematics.

E_{beam} (GeV)	θ_e (°)	θ_{pq} (°)
0.843	100.7	0, 8, 16
1.643	37.2	0, ± 8
2.442	23.4	0, ± 2.5 , ± 8 , ± 16 , ± 20

The systematic uncertainty in cross section measurements is about 5%. This uncertainty is dominated by the uncertainty in the ${}^1\text{H}(e, e)$ cross section to which the data were normalized [28].

Figure 1 shows the measured cross section as a function of missing energy at $E_{\text{beam}} = 2.4$ GeV for various proton angles, $2.5^\circ \leq \theta_{pq} \leq 20^\circ$. The average missing momentum increases with θ_{pq} from 50 to 340 MeV/c. The prominent peaks at 12 and 18 MeV are due to $1p$ -shell proton knockout and are described in [21], where it was shown that they can be explained up to $P_m = 340$ MeV/c by relativistic distorted wave impulse approximation (DWIA) calculations. However, the spectra for $E_m > 20$ MeV exhibit very different behavior. At the lowest missing momentum, $P_m \approx 50$ MeV/c, the wide peak centered at $E_m \approx 40$ MeV is due predominantly to knockout of $1s_{1/2}$ -state protons. This peak is less prominent at $P_m \approx 145$ MeV/c and has vanished beneath a flat background for $P_m \geq 200$ MeV/c. At $E_m > 60$ MeV or

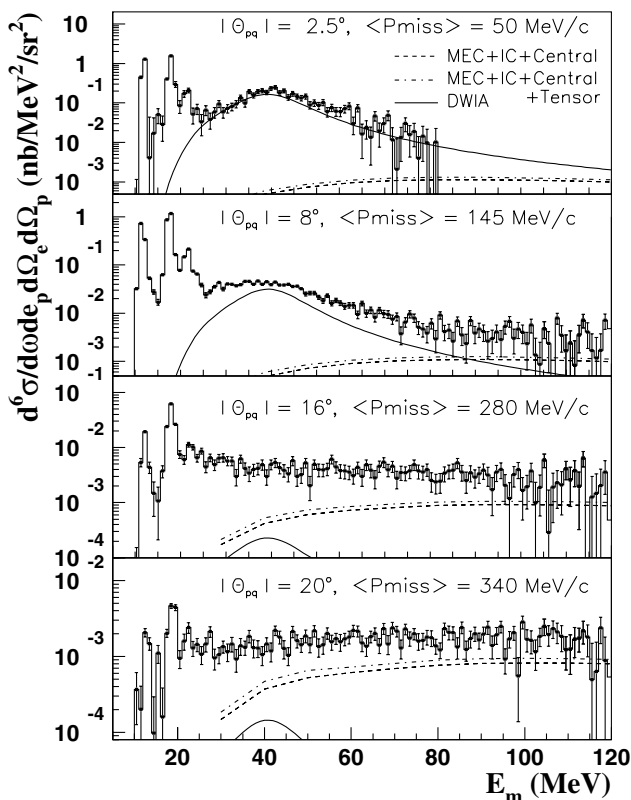


FIG. 1. Average cross sections measured at different outgoing proton angles as a function of missing energy. The cross section shown at each angle is the average between the cross sections measured at either side of \vec{q} at that angle. The curves show the s -shell single-particle strength calculated by Kelly folded with the Lorentzian parametrization of Mahaux. The dashed line shows the Ryckebusch *et al.* calculations of the $(e, e'pn)$ and $(e, e'pp)$ contributions to $(e, e'p)$ including meson-exchange currents (MEC), intermediate Δ creation (IC), and central correlations, while the dot-dashed line also includes tensor correlations.

$P_m > 200$ MeV/c, the cross section does not depend on E_m and decreases only weakly with P_m .

We compared our $E_m > 25$ MeV results to single-particle knockout calculations by Kelly [29] to determine how much of the observed cross section can be explained by $1s_{1/2}$ -state knockout. Kelly performed DWIA calculations using a relativized Schrödinger equation in which the dynamical enhancement of lower components of Dirac spinors is represented by an effective current operator [30]. For the $1s_{1/2}$ state, Kelly used a normalization factor of 0.73 with respect to the single-particle strength and spread the cross section and the response functions over missing energy using the Lorentzian parametrization of Jeukenne and Mahaux [31].

At small P_m , where there is a clear peak at 40 MeV, this model describes the cross section (see Fig. 1) and the separated R_L and R_T responses well [24]. The extracted magnitude of $(S_T - S_L)$ [24] is consistent with the decrease in $(S_T - S_L)$ with Q^2 seen in the measurements of Ulmer *et al.* [7] at $Q^2 = 0.14$ (GeV/c) 2 and by Dutta [16] at $Q^2 = 0.6$ and 1.8 (GeV/c) 2 . This suggests that, in parallel kinematics, transverse non-single-nucleon knockout processes decrease with Q^2 . At larger P_m , where there is no peak at 40 MeV, the DWIA cross section is much smaller than the data (see Fig. 1). Relativistic DWIA calculations by other authors [32,33] show similar results. This confirms the attribution of the large missing momentum cross section to non-single-nucleon knockout.

Figure 1 also shows $(e, e'pn)$ and $(e, e'pp)$ contributions to the $(e, e'p)$ cross section calculated by Ryckebusch *et al.* [34] in a Hartree-Fock (HF) framework. The cross section for the two particle knockout has been calculated in the “spectator approximation” assuming that the two nucleons escape from the residual $A - 2$ system without being subject to inelastic collisions with other nucleons. This calculation includes pion exchange currents, intermediate Δ creation, and central and tensor short-range correlations. According to this calculation, in our kinematics, two-body currents (pion-exchange and Δ) account for approximately 85% of the calculated $(e, e'pn)$ and $(e, e'pp)$ strength. Short-range tensor correlations contribute approximately 13% while short-range central correlations contribute only about 2%. Since the two-body currents are predominantly transverse, the calculated $(e, e'pn)$ and $(e, e'pp)$ cross section is mainly transverse. The flat cross section predicted by this calculation for $E_m > 50$ MeV is consistent with the data, but it accounts for only about half the measured cross section. Hence, additional contributions to the cross section such as heavier meson exchange and processes involving more than two hadrons must be considered.

Figures 2 and 3 present the separated response functions for various proton angles. Because of kinematic constraints, we were able to separate only the responses for $E_m < 60$ MeV. The separated response functions can be used to check the reaction mechanism. If the excess continuum strength at high P_m is dominated by two-body

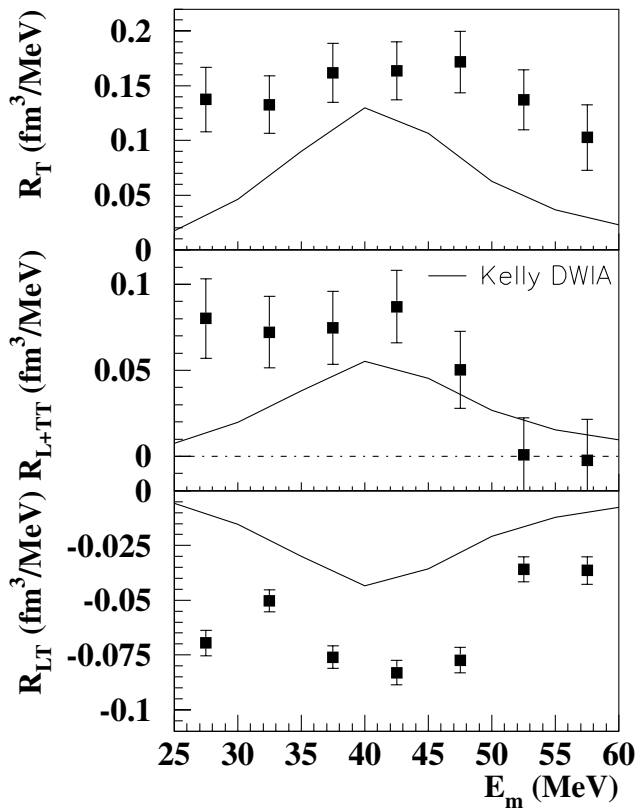


FIG. 2. Response functions for $\langle P_m \rangle \approx 145 \text{ MeV}/c$. The calculations have been folded with the Lorentzian parametrization of Mahaux and have been binned in the same manner as the data.

currents rather than by correlations, then it should be predominantly transverse.

Figure 2 presents the separated response functions (R_{L+TT} , R_T , and R_{LT} ; $R_{L+TT} \equiv R_L + \frac{V_{TT}}{V_L} R_{TT}$) for $|\theta_{pq}| = 8^\circ$ ($\langle P_m \rangle \approx 145 \text{ MeV}/c$). The Mahaux parametrization does not reproduce the shape of R_L or of R_T as a function of missing energy. For $E_m > 50 \text{ MeV}$, R_{L+TT} (which is mainly longitudinal because $\frac{V_{TT}}{V_L} R_{TT}$ is estimated to be only about 7% of R_L [29] in these kinematics) is consistent with both zero and with the calculations. R_T , on the other hand, remains nonzero to at least 60 MeV. R_T is also significantly larger than the DWIA calculation. R_{LT} is about twice as large as the DWIA calculation over the entire range of E_m . R_{LT} is nonzero for $E_m > 50 \text{ MeV}$, indicating that R_L is also nonzero in that range.

Figure 3 presents the separated response functions for $|\theta_{pq}| = 16^\circ$ ($\langle P_m \rangle \approx 280 \text{ MeV}/c$). At this missing momentum, none of the measured response functions show a peak at $E_m \approx 40 \text{ MeV}$ where single-particle knockout from the $1s_{1/2}$ state is expected. R_{L+TT} is close to zero and the DWIA calculation. However, R_T and R_{LT} are much larger than the DWIA calculation. R_T is also much larger than R_{LT} indicating that the cross section is due in large part to transverse two-body currents. The fact that R_{LT} is

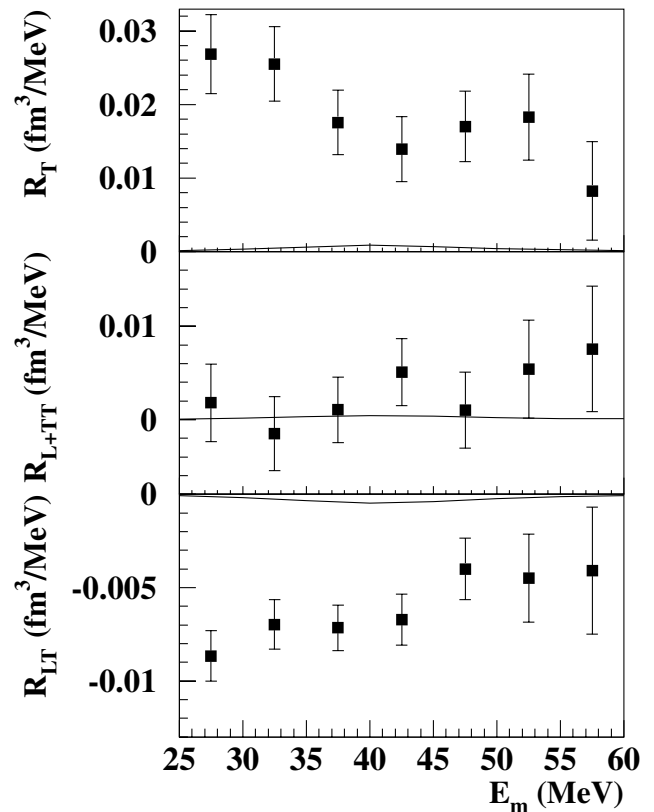


FIG. 3. Response functions for $\langle P_m \rangle \approx 280 \text{ MeV}/c$.

nonzero indicates that R_L , although too small to measure directly, is also nonzero.

To summarize, we have measured the cross section and response functions (R_L , R_T , and R_{LT}) for the $^{16}\text{O}(e, e'p)$ reaction in quasielastic kinematics at $Q^2 = 0.8 \text{ (GeV}/c)^2$ and $\omega = 439 \text{ MeV}$ for missing energies $25 < E_m < 120 \text{ MeV}$ at various missing momenta $P_m \leq 340 \text{ MeV}/c$. For $25 < E_m < 50 \text{ MeV}$ and $P_m \approx 60 \text{ MeV}/c$ the reaction is dominated by single-nucleon knockout from the $1s_{1/2}$ state and is described well by DWIA calculations.

At increasing missing momenta, the importance of the single-particle aspects is diminished. The cross section and the response functions no longer peak at the maximum of the s shell (40 MeV). They no longer have the expected s -shell Lorentzian shape. DWIA calculations [29] underestimate the cross section and response functions at $P_m > 200 \text{ MeV}/c$ by more than a factor of 10. Hence, we conclude that the single-particle aspect of the $1s_{1/2}$ state contributes less than 10% to the cross section at $P_m > 200 \text{ MeV}/c$. This is in contrast to the p shell, where DWIA calculations describe the data well up to $P_m = 340 \text{ MeV}/c$.

At $25 < E_m < 120$ and $P_m > 200 \text{ MeV}/c$ the cross section is almost constant in missing energy and missing momentum. For $E_m > 60 \text{ MeV}$ this feature is well reproduced by two-nucleon knockout calculations, $(e, e'pp)$ plus $(e, e'pn)$. These calculations also account for the

predominantly transverse nature of the cross section. The transversity of the cross section and the calculations suggest that two-body currents (such as MEC and IC) contribute significantly to the excess continuum strength at high P_m . At least according to this model, these contributions are much larger than those from correlations. To our knowledge, this is the only model which can account for the shape, transversity, and about half of the magnitude of the measured continuum cross section. The unaccounted for strength suggests that additional currents and processes play an important role.

We acknowledge the outstanding support of the staff of the Accelerator and Physics Divisions at Jefferson Laboratory that made this experiment successful. We thank Dr. J. Ryckebusch for theoretical calculations. We also thank Dr. J. M. Udias for providing the NLSH bound-state wave functions. This work was supported in part by the U.S. Department of Energy Contract No. DE-AC05-84ER40150 under which the Southeastern Universities Research Association (SURA) operates the Thomas Jefferson National Accelerator Facility, other Department of Energy contracts, the National Science Foundation, the Italian Istituto Nazionale di Fisica Nucleare (INFN), the French Atomic Energy Commission and National Center of Scientific Research, and the Natural Sciences and Engineering Research Council of Canada.

-
- [1] The kinematical quantities are as follows: the electron scattered at angle θ_e transfers momentum \vec{q} and energy ω with $Q^2 = \vec{q}^2 - \omega^2$. The ejected proton has mass m_p , momentum \vec{p}_p , energy E_p , and kinetic energy T_p . The cross section is typically measured as a function of missing energy $E_m = \omega - T_p - T_{\text{recoil}}$ and missing momentum $P_m = |\vec{q} - \vec{p}_p|$. The polar angle between the ejected proton and virtual photon is θ_{pq} , and the azimuthal angle is ϕ . $\theta_{pq} > 0^\circ$ corresponds to $\phi = 180^\circ$ and $\theta_p > \theta_q$. $\theta_{pq} < 0^\circ$ corresponds to $\phi = 0^\circ$.
- [2] A. S. Raskin and T. W. Donnelly, *Ann. Phys. (N.Y.)* **191**, 78 (1989).

- [3] J. J. Kelly, *Adv. Nucl. Phys.* **23**, edited by J. W. Negele and E. Vogt, 75 (1996), and references therein.
- [4] U. Amaldi *et al.*, *Phys. Lett.* **25B**, 24 (1967).
- [5] J. Mougey *et al.*, *Nucl. Phys.* **A262**, 461 (1976).
- [6] S. Frullani and J. Mougey, *Adv. Nucl. Phys.* **14**, edited by J. W. Negele and E. Vogt, 1 (1984), and references therein.
- [7] P. E. Ulmer *et al.*, *Phys. Rev. Lett.* **59**, 2259 (1987).
- [8] R. Lourie *et al.*, *Phys. Rev. Lett.* **56**, 2364 (1986).
- [9] L. Weinstein *et al.*, *Phys. Rev. Lett.* **64**, 1646 (1990).
- [10] J. H. Morrison *et al.*, *Phys. Rev. C* **59**, 221 (1999).
- [11] M. Holtrop *et al.*, *Phys. Rev. C* **58**, 3205 (1998).
- [12] T. de Forest, *Nucl. Phys.* **A392**, 232 (1983).
- [13] T. de Forest, *Ann. Phys. (N.Y.)* **45**, 365 (1967).
- [14] J. B. J. M. Lanen *et al.*, *Phys. Rev. Lett.* **64**, 2250 (1990).
- [15] G. van der Steenhoven *et al.*, *Nucl. Phys.* **A480**, 547 (1988).
- [16] D. Dutta, Ph.D. thesis, Northwestern University, 1999 (unpublished).
- [17] J. Ryckebusch *et al.*, *Nucl. Phys.* **A624**, 581 (1997).
- [18] A. Gil *et al.*, *Nucl. Phys.* **A627**, 599 (1997).
- [19] T. Takaki, *Phys. Rev. C* **39**, 359 (1989).
- [20] A. Saha, W. Bertozzi, R. W. Lourie, and L. B. Weinstein, Jefferson Laboratory Proposal No. 89-003, 1989; K. G. Fissum, MIT-LNS Internal Report No. 02, 1997.
- [21] J. Gao *et al.*, *Phys. Rev. Lett.* **84**, 3265 (2000).
- [22] F. Garibaldi *et al.*, *Nucl. Instrum. Methods Phys. Res., Sect. A* **314**, 1 (1992).
- [23] www.jlab.org/Hall-A/equipment/HRS.html
- [24] N. Livanage, Ph.D. thesis, MIT, 1999 (unpublished).
- [25] E. Quint, Ph.D. thesis, University of Amsterdam, 1988 (unpublished).
- [26] www.physics.odu.edu/~ulmer/mceep/mceep.html; see also J. A. Templon *et al.*, *Phys. Rev. C* **61**, 014607 (2000).
- [27] E. Borie and D. Drechsel, *Nucl. Phys.* **A167**, 369 (1971).
- [28] G. G. Simon *et al.*, *Nucl. Phys.* **A333**, 381 (1980); L. E. Price *et al.*, *Phys. Rev. D* **4**, 45 (1971).
- [29] J. J. Kelly, *Phys. Rev. C* **60**, 044609 (1999).
- [30] M. Hedayati-Poor, J. I. Johansson, and H. S. Sherif, *Phys. Rev. C* **51**, 2044 (1995).
- [31] J. P. Jeukenne and C. Mahaux, *Nucl. Phys.* **A394**, 445 (1983).
- [32] A. Picklesimer, J. W. Van Orden, and S. J. Wallace, *Phys. Rev. C* **32**, 1312 (1985).
- [33] J. M. Udiás *et al.*, *Phys. Rev. Lett.* **83**, 5451 (1999).
- [34] S. Janssen *et al.*, *Nucl. Phys.* **A672**, 285 (2000).